Comparison of semi-empirical potential functions for silicon and germanium

Stephen J. Cook* and Paulette Clancy†
School of Chemical Engineering, Cornell University, Ithaca, New York 14853
(Received 7 July 1992)

We report the results of investigations into the behavior of the crystalline and liquid phases of silicon and germanium as they are modeled by the Tersoff and modified-embedded-atom-method (MEAM) potentials. The structure of the solid-liquid interface produced by each potential is determined, as are the melting points corresponding to each potential model. The equilibrium properties of both crystalline and liquid silicon and germanium as modeled by the Tersoff and MEAM potentials are then presented. The Tersoff potential is found to overestimate greatly the melting point of both silicon and germanium, while the MEAM underestimates the melting point of silicon by approximately 15%. The MEAM does not yield a stable liquid phase of germanium. Both potential models produce a (100) solid-liquid interface for both semiconductors that is rough, while the (111) interface is found to be atomically smooth. The Tersoff potential yields an amorphous phase for both silicon and germanium, but efforts to produce an amorphous MEAM phase were unsuccessful. Rapid solidification of MEAM silicon produced unphysical regrowth velocities.

I. INTRODUCTION

Laser annealing techniques are being considered once again as viable processing techniques for the production of compound semiconductor materials, such as alloys of silicon and germanium. Silicon-germanium alloys present a materials processing challenge in that misfit dislocations will form if the material is held at elevated temperatures for an extended period of time. This problem has been remedied at least in part by the introduction of a technique that combines molecular-beam or vapor-phase epitaxy with laser annealing.[1–3] This method, which is still under development, is receiving increasing attention and holds promise for the production of compound semiconducting materials. Mechanisms which might mediate this growth or limit the germanium concentration, however, are still completely unknown.

Although great progress has been made toward developing *ab initio* simulation methods, such as the Car-Parrinello method,[4–6] for atomic-scale studies for semiconductors, these methods are still far too computationally demanding to allow large-scale studies. This limitation is particularly important in atomic-scale investigations of materials processing phenomena such as liquid-phase epitaxy. This has led several groups to propose computationally efficient empirical potential models for silicon that could be used for this or similar purposes.[7–21] Although there have been many efforts to produce a reliable empirical potential for crystalline silicon, only the Stillinger-Weber potential was parametrized by also considering liquid-phase properties. Of the potentials that were not fitted to liquid-phase properties, only Tersoff[20] has reported *any* results relating to the liquid phase. Tersoff, moreover, only reported an estimate of the melting temperature and the structure of the liquid as determined by the radial distribution function. Although there are many potential models for silicon, only the Tersoff and modified-embedded-atom-method (MEAM) potentials have been extended to germanium. Ding and Andersen suggested that germanium might also be modeled by the Stillinger-Weber potential with appropriately scaled length and energy parameters.[22] The quality of the germanium potentials is almost completely untested.

In order to investigate the suitability of these potentials for studies of materials processing phenomena involving disordered phases, we have performed investigations of the phase behavior of the Tersoff and MEAM potentials using equilibrium molecular-dynamics techniques.

II. POTENTIAL MODELS

The Stillinger-Weber potential utilizes both two-body and three-body interaction terms to stabilize the diamond cubic structure of crystalline silicon and is given as

$$\phi(\mathbf{r})=\sum_{\substack{i,j\\ j>i}}\phi_2(r_{ij})+\sum_{\substack{i,j,k\\ k>j>i}}\phi_3(r_{ij},r_{ik},\cos\theta_{ijk})\ , \tag{1}$$

$$\phi_2(r)=A\epsilon\left[B\left[\frac{\sigma}{r}\right]^p-\left[\frac{\sigma}{r}\right]^q\right]\exp\left[\frac{\sigma}{r-a}\right]\ , \tag{2}$$

$$\phi_3(r_{ij},r_{ik},\cos\theta_{ijk})=\lambda\epsilon\exp\left[\frac{\gamma\sigma}{r_{ij}-a}\right]\times\exp\left[\frac{\gamma\sigma}{r_{ik}-a}\right]\left[\cos\theta_{ijk}+\frac{1}{3}\right]^2\ , \tag{3}$$

where A, B, p, q, λ, and γ are adjustable parameters and a is a cutoff radius at which the potential goes smoothly to zero. The parameters in the potential were adjusted to reproduce the properties of both crystalline and liquid silicon.

The Tersoff potential is written as a Morse pair potential and includes many-body effects by specifying that the

coefficients of the Morse terms be dependent on the local environment of a specific atomic pair. Tersoff gives his potential as[20]

$$\sigma(\mathbf{r})=\sum_{i\neq j} V_{ij} \ , \tag{4}$$

where

$$V_{ij}=f_c(r_{ij})[\,A_{ij}\exp(-\lambda_{ij}r_{ij})-b_{ij}B_{ij}\exp(-\mu_{ij}r_{ij})\,] \tag{5}$$

and

$$b_{ij}=\chi_{ij}(1+\beta_i^{n_i}\zeta_{ij}^{n_i})^{-1/2n_i} \ , \tag{6}$$

$$\zeta_{ij}=\sum_{k\neq i,j} f_c(r_{ij})g(\theta_{ijk})\exp[\lambda_3^3(r_{ij}-r_{ik})] \ , \tag{7}$$

$$g(\theta_{ijk})=1+\frac{c_i^2}{d_i^2}-\frac{c_i^2}{d_i^2+(h_i-\cos\theta_{ijk})^2} \ . \tag{8}$$

Tersoff later modified his potential slightly by suggesting that setting $\lambda_3=0$ had little effect on the quality of the potential.[21] This simplification has been adopted in this work. The function $f_c(r_{ij})$ is a cutoff function that changes smoothly from unity to zero within a thin, specified cutoff shell. The adjustable parameters A, B, λ, μ, β, n, c, d, h, R, and S were fitted to a large database of energies determined by *ab initio* calculations for a variety of real and hypothetical structures, and the subscript ij indicates that the parameter depends on the identity of atoms i and j. Tersoff apparently did not fit to any liquid-phase data. Parameters are given for carbon, silicon, germanium, and their alloys.

The modified-embedded-atom method[9] is a more general form of the embedded-atom method (EAM), which is a very successful potential model for face-centered-cubic metals. The EAM was developed by Daw and Baskes for pure metals[23,24] and extended to alloy systems by Foiles *et al.*[25–27] Embedded-atom-like potentials have also been offered by Oh and Johnson,[28–32] Chen, Srolovitz, and Voter,[33] and Finnis and Sinclair.[34] The EAM methodology expresses the energy of a system of interacting atoms as the sum of the energy required to "embed" an atom in an electron gas whose density is determined by the other atoms in the system, and a pair potential, which provides a correction term related to ion-ion interactions. The EAM total energy is given as

$$E=\sum_i F(\rho_i)+\sum_{i,j>i}\phi_{ij}(r_{ij}) \ , \tag{9}$$

where ρ_i is the total electron density at atom i due to all other atoms in the system, F is the embedding function, and ϕ_{ij} is the pair potential correction term. EAM studies of metals assume that the electron density ρ_i can be expressed as a pairwise summation of radially symmetric electron densities from the other atoms in the system

$$\rho_i^{\mathrm{EAM}}=\sum_{i,j\neq i}\rho_{ij}^a \ . \tag{10}$$

Baskes, Nelson, and Wright have shown that this assumption is invalid for silicon[9] and that higher-order multibody terms must be included in the electron-density calculation to account for bond-bending interactions:

$$\rho_i=\sum_j \rho^2(r_{ij})+\sum_j\sum_k \rho^3(\mathbf{r}_{ij},\mathbf{r}_{ik},\mathbf{r}_{jk}) \ , \tag{11}$$

where ρ^2 and ρ^3 signify the two-body and three-body contributions to the electron density. Baskes, Nelson, and Wright expand the three-body term as a sum of Legendre polynomials and arrive at the expression

$$\rho_i^{\mathrm{MEAM}}=\sum_j \rho_j^a(r_{ij})+\sum_j\sum_k [a_j^1 a_k^1\cos\theta_{ijk}-a_j^2 a_k^2(1-3\cos^2\theta_{ijk})]\rho_j^a(r_{ij})\rho_k^a(r_{ik}) \ . \tag{12}$$

The constants a^1 and a^2 are adjustable parameters,[35] θ_{ijk} is the angle between atoms i, j, and k subtended at atom i, and ρ_j^a is the radially symmetric two-body electron-density expression that is termed ρ^2 in Eq. (11) above.

The authors of the MEAM further restrict the total cohesive energy of the crystalline phase of silicon or germanium to be given by an equation of state developed by Rose *et al.*,[36] which is similar in form to that used in the development of the Tersoff potential. Unlike EAM models for metals, the MEAM pair potential is calculated by assuming a functional form for the embedding function and then calculating the pair potential necessary to bring the system energy to the value required by the equation of state. No liquid-phase properties were used to fit the potential.

The Tersoff and MEAM potentials for silicon and germanium have been used to obtain information about both the bulk phases of solid and liquid silicon and germanium, as well as to characterize the nature of both the equilibrium and rapidly crystallizing solid-liquid interfaces. These data, which will be presented in the following sections, have been compared to data obtained from the Stillinger-Weber potential, as well as to existing experimental data.

III. EQUILIBRIUM SOLID-LIQUID INTERFACES OF SILICON

The phase behavior of silicon and germanium as modeled by the Tersoff and MEAM potentials has been examined using a variety of molecular-dynamics (MD) codes. The melting point and solid-liquid interfaces were studied using a method similar to that used by Landman *et al.*[37] to study the solid-liquid interface of Stillinger-Weber silicon. The periodic boundary condition in the direction normal to the desired surface was removed and replaced by a free surface that prevented the superheating commonly found in bulk simulations of melting behavior. Several atomic planes on the bottom of the cell, corresponding to a distance slightly greater than the cutoff of the potential in use, were fixed in their bulk positions to emulate the presence of an underlying bulk

phase. Periodic boundary conditions were applied in the two transverse directions and a time step of 1 fs was used for the Stillinger-Weber and MEAM potentials. A time step of 0.2 fs was used in simulations of the Tersoff potential. Although the larger time step of 1 fs was sufficient to maintain energy conservation during simulation of crystalline silicon using the Tersoff potential, it was not sufficient for simulations of the liquid phase. Energy conservation using the specified time steps was excellent, with a variation of no more than 10^{-4} eV/atom in total energy throughout the approximately 150 ps simulation time necessary to obtain equilibrium solid-liquid interfaces for each potential. The simulation cell used to study the (100) orientations of each potential contained 50 atoms/plane, for a total of 2000 atoms, while that used to study the (111) orientations contained 160 atoms per (111) doublet. The total system size for studies of the (111) orientation was 2400 atoms. The atoms above the fixed lattice were either thermostated for isothermal (*NVT*) conditions or allowed to interact via Newtonian dynamics under conditions of constant total energy (*NVE*). The method of Landman *et al.* can be used to find the melting point of a material in the following way. An interfacial configuration exposing the desired crystalline orientation is first created with a system density corresponding to zero applied pressure at a temperature that is expected to be below but near the melting point of the material. The configuration is equilibrated at this temperature for a short time, the temperature scaling is turned off, and energy is added to the cell so that approximately half of the solid melts. The resulting configuration is an adiabatic system comprised of approximately equal parts of solid and liquid that are in equilibrium at the melting temperature. If the final temperature is very different from the original estimate, the density of the cell may be adjusted. A further simulation period would then be necessary to allow the system to reach equilibrium.

The procedure described above was used to determine the melting points of MEAM, Tersoff, and Stillinger-Weber silicon. No data yet exist for the liquid phase of the MEAM semiconductors, and it is of interest to determine how well these potentials might reproduce disordered semiconductor phases. Although Tersoff estimated the melting point of his potential to be 3000 ± 500 K,[20] he does not describe the method used to make this determination. It is of interest, therefore, to calculate this value independently. The melting point of the Stillinger-Weber potential is already well known. Recalculation of the melting point, therefore, provides a check on the accuracy of the computer program used and provides data on the Stillinger-Weber solid-liquid interface that may be used for comparison with those produced by the other potentials.

Since it was desirable to have Stillinger-Weber interfacial configurations with which to compare the results obtained from other potential models, and also to check our method and simulation code for errors, the method described above was used to produce an equilibrium solid-liquid interface on both the (100) and (111) orientations of the Stillinger-Weber solid. This simulation was performed by Landman *et al.* in 1986,[37] who obtained an estimate of the melting point of 1665 K. Later work by Broughton and Li showed the true melting point to be 1691 K, which is in very good agreement with the experimental value of 1683 K.[38] The value obtained by Landman *et al.* thus had an error of 1%. Study of the Stillinger-Weber system began here with the creation of a crystalline configuration whose density was set to that reported by Broughton and Li for a reduced temperature of 0.065, which may be compared to the reduced melting temperature of 0.0672. Melting was initiated on both orientations using the method of Chokappa, Cook, and Clancy.[39] Melting initiated at the crystal-vacuum surface in both systems and the solid-liquid interface proceeded into the solid until the average reduced temperature in both simulation cells was 0.0671 ± 0.0011 (1688 ± 26 K). This process took approximately 150 ps (150 000 MD time steps) for both surface orientations studied. The excellent agreement between the value obtained here and that reported by Broughton and Li validates the method and simulation code that we have employed.

The melting point and interfacial morphology of Tersoff silicon was also studied using the method of Landman *et al.* The system size employed was equal in size to that used for the Stillinger-Weber (SW) potential. An interfacial configuration exposing the (100) orientation was created and equilibrated for 50 000 MD time steps (10 ps) at a temperature of 1500 K. The system density was set to that of the crystal at 1500 K under conditions of no externally applied stress, i.e., zero pressure. This value was obtained using an isothermal-isobaric (*NPT*) molecular-dynamics simulation code. Energy was added to the system using the method of energy carriers described in Ref. 39. Melting initiated at the vacuum surface and proceeded into the solid until the system temperature fell to a value of 2744 ± 42 K. Since the steady-state temperature was so different from the original starting temperature, a new interfacial configuration was created and equilibrated at a temperature of 2500 K. The melting process was repeated and a lengthy simulation run of 700 000 MD time steps (140 ps) revealed the equilibrium melting point to be 2547 ± 22 K. The large change in the estimate of the melting point was caused by an insufficiently long simulation time for the first attempt. Although the number of time steps required to reach steady state has increased by a factor of 4 over SW, the amount of "real" time required has remained constant. The additional effort is only required because the time step used in studies of the Tersoff system is smaller. The (100) solid-liquid interface of Tersoff silicon is very diffuse, and shows the presence of interplanar defects all the way down to the static lattice. Figure 1 shows the nature of the (100) solid-liquid interface of Tersoff silicon, along with that of the Stillinger-Weber potential. Although the actual melting point of the potential, 2547 K, is somewhat better than that estimated previously by Tersoff, it is still almost 900 K higher than the experimental melting point of silicon. The value is in error by 51%. Due to the large error in the melting point, no study was made of the Tersoff (111) solid-liquid interface.

The melting point of MEAM silicon was calculated on

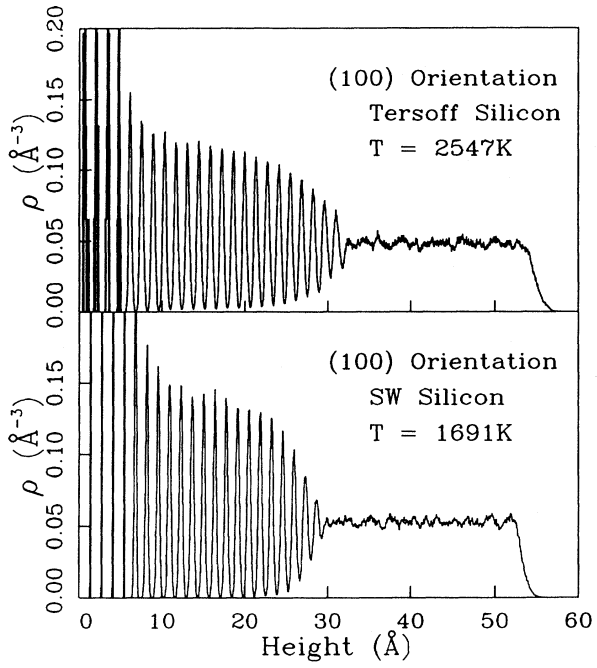

FIG. 1. Density profiles comparing the morphology of the (100) solid-liquid interface of silicon as predicted by the modified-Tersoff and Stillinger-Weber potentials.

both the (100) and (111) orientations using the same method as was used for the Stillinger-Weber and Tersoff potentials. An initial estimate of 1000 K was used as the starting point for the determination of the melting point, and the initial density of the atoms in the simulation cell was set to the zero-pressure density for crystalline MEAM silicon at 1000 K. The cell was then equilibrated at constant temperature for 50 000 time steps (50 ps), the temperature scaling was turned off, and then enough energy was added to the cell to cause approximately half of it to melt. Melting initiated at the surface and continued until enough of the crystal had melted to cause the system temperature to fall to a constant value. The average temperature for both orientations stabilized at 1445±25 K after a simulation time of 120 ps. The zero-pressure density of MEAM crystalline silicon at 1445 K was then calculated and the size of the simulation cell was adjusted to this value. Equilibration of the (100) solid-liquid interface was then continued for another 120 ps. Observation of the average system temperature during the three 40 ps sections of this latter 120 ps indicated that the system had relaxed to the new temperature of 1475±25 K after only the first 40 ps of this latter equilibration period. Although this procedure could be repeated yet again with the density for the higher temperature, calculation of the zero-pressure density at 1475 K showed that the system was only under a 0.05% strain when using the density appropriate for 1445 K at the higher temperature. This may be compared to a mismatch of 0.6% between the lattice constants appropriate for 1445 and 1000 K. Since any feature change in the temperature was likely to have been less than the statistical error of the simulation data, the procedure was stopped at this point. The value of the MEAM melting point for crystalline silicon was then taken to be 1475±25 K. The underestimation of the melting point of silicon observed here is consistent with previous investigations of the melting points of transition metals as modeled by the EAM.[40] Foiles and Adams found that the EAM usually predicted the melting points of the transition metals to be at or below the values that are observed experimentally.

An attempt was made to use the same procedure of changing the system density for the (111) solid-liquid interface as had been used for the (100) orientation, but a simple change of the width of the simulation cell produced no subsequent change in temperature after 80 ps. Subsequent attempts to produce interface motion by turning on the "heat bath" portion of the simulation cell showed that the solid-liquid interface was immobile on simulation time scales at system temperatures at least as low as 1350 K, which represents an undercooling of almost 10%. This phenomenon is caused by the nature of the (111) solid-liquid interface, which is atomically smooth. Regrowth on this interface, like on the (111) interface of the Lennard-Jones potential, requires the initial nucleation of atoms onto existing crystal to form a new layer. Our finding does not indicate a specific deficiency of the MEAM potential, only that nucleation is a slow process that is difficult to capture in a molecular-dynamics simulation. This is especially true for the (111) interface. The equilibrium (111) solid-liquid interface was obtained by simply scaling system velocities back to 1475 K and equilibrating the system for 80 ps before collecting

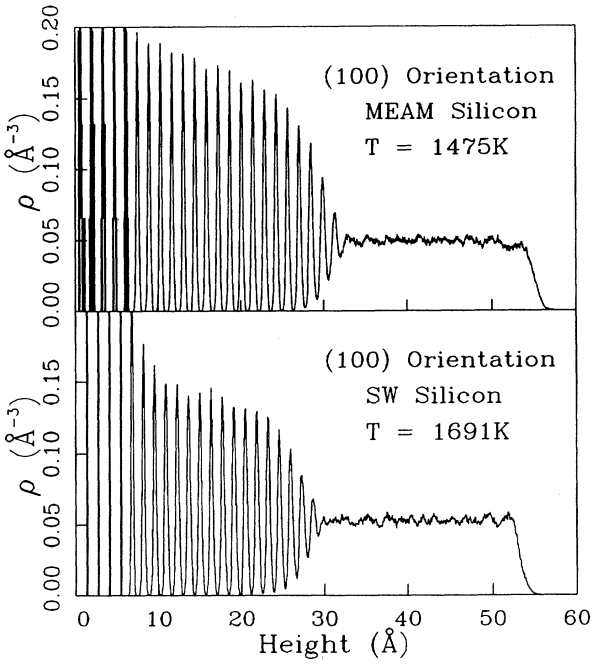

FIG. 2. Density profiles comparing the morphology of the solid-liquid interface on the (100) orientation of silicon as produced by the MEAM and Stillinger-Weber potentials.

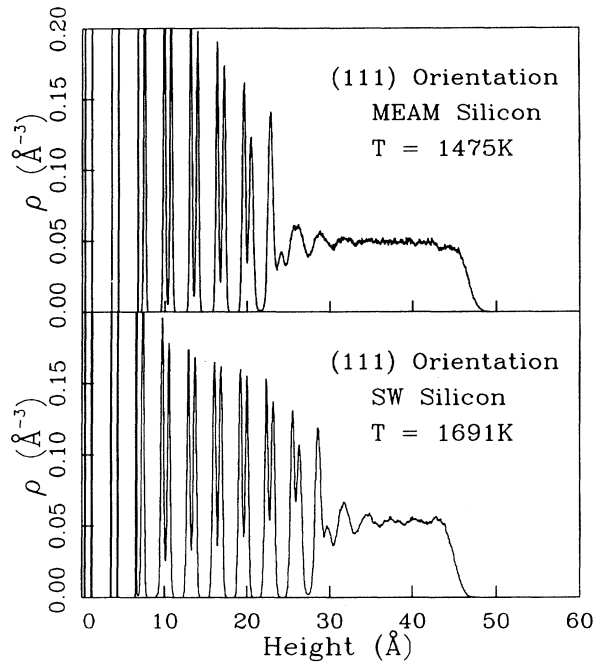

FIG. 3. Density profiles comparing the morphology of the solid-liquid interface on the (111) orientation of silicon as produced by the MEAM and Stillinger-Weber potentials.

averages.

The spatial variation of the MEAM and Stillinger-Weber interfaces is shown in Figs. 2 and 3, where the singlet density profiles obtained from the MEAM are compared to those obtained from SW. The density profiles are remarkably similar, showing a broad and rough interface on (100) and the sharp, abrupt interface characteristic of (111). There is also no evidence of "layering" or ordering in the liquid region adjacent to the (111) solid, with the exception of the very pronounced peak showing ordering of the liquid atoms immediately in contact with crystal on (111).

IV. PHASE DIAGRAMS FOR TERSOFF AND MEAM SILICON

Information concerning the crystalline and liquid branches of the equilibrium phase diagram of both the Tersoff and MEAM semiconductors was obtained using an isothermal-isobaric (*NPT*) molecular-dynamics simulation code that employed the modified leap-frog algorithm of Brown and Clarke.[41] The simulation cell was cubic and periodic boundary conditions were applied in all three Cartesian directions. Ensemble averages were calculated using a system comprised of 1000 atoms. Studies of the MEAM semiconductors were conducted using a time step of 1 fs, while the time step in simulations of the Tersoff systems was 0.2 fs. Studies of the crystalline configurations for each semiconductor system begun at low temperature with a perfect diamond lattice as an initial atomic configuration. The system was equilibrated for at least 50 000 time steps (50 ps for the MEAM) and averages were then collected for at least another 50 000 time steps (50 ps). Simulation of the solid at a higher temperature was then begun with the resulting atomic configuration of the previous lower-temperature study. This process was continued until melting of the crystal occurred. The resulting liquid configuration was then equilibrated for at least 100 000 time steps at a temperature 500 K above the temperature at which melting occurred, thus assuring that no residual solid structure remained. Studies of the liquid phase began at this point. Each liquid state point was obtained by the same equilibration and averaging process as for the solid, except that the system temperature was systematically reduced from the highest temperature configuration studied. Studies of the crystalline phase of both Tersoff and MEAM silicon were started at a temperature of 500 K, and each state point in the solid phase was obtained by instantaneously increasing the system temperature in the manner just described. Each liquid state point was obtained by instantaneously decreasing the system temperature below the previous configuration temperature. All simulations were performed under conditions of zero externally applied pressure.

A. Equilibrium phases

The densities and configurational energies of crystalline and liquid Tersoff silicon are shown in Figs. 4 and 5, while data for MEAM silicon are shown in Figs. 6 and 7. The crystalline phase produced by each potential exhibits a nearly linear decrease in density and increase in energy until it finally reaches the limit of superheating and melts, which occurs between 1750 and 2000 K for the MEAM

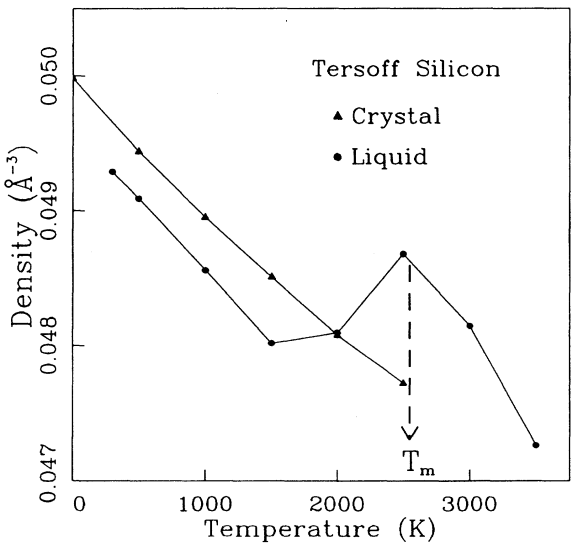

FIG. 4. The density of silicon in the solid and liquid phases as represented by the modified-Tersoff potential. Data were collected along the isobar corresponding to zero average pressure.

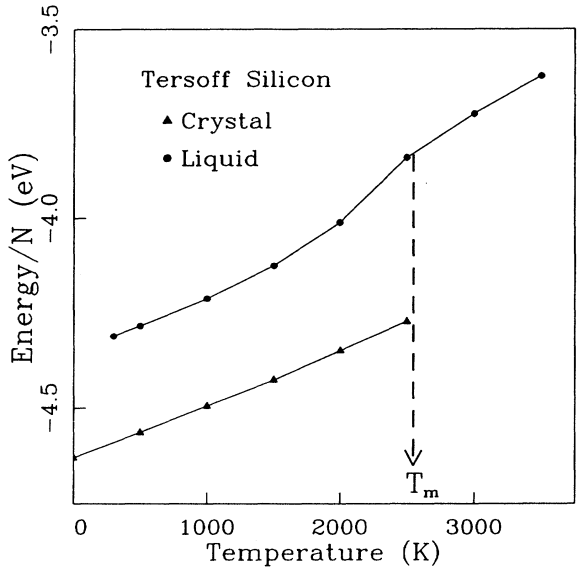

FIG. 5. The configurational energy per atom of silicon in the solid and liquid phases as represented by the modified-Tersoff potential. Data were collected along the isobar corresponding to zero average pressure.

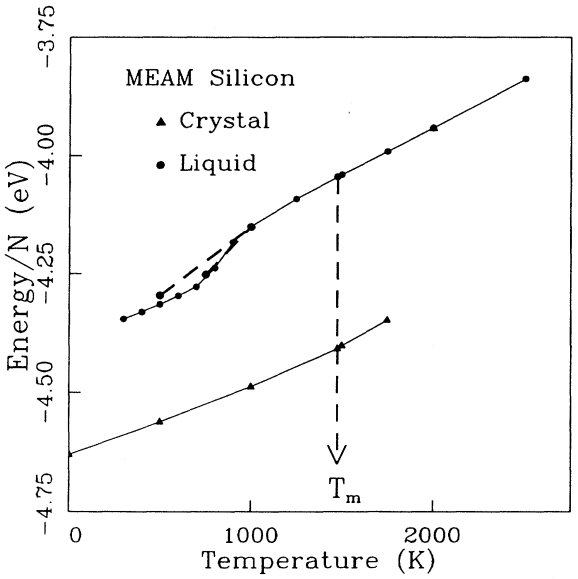

FIG. 7. The configurational energy per atom of silicon in the solid and liquid phases as represented by the modified-embedded-atom Method. Dashed lines indicate instantaneous quenches to metastable states from an initial temperature of 900 K. Data points on the solid line, which represents the liquid branch at temperatures below 900 K, represent values calculated by cooling the liquid at the rate of 10^{12} K/s, followed by equilibration and averaging. Data were collected along the isobar corresponding to zero average pressure.

and between 2500 and 3000 K for Tersoff. This represents a superheating of at least 21% for the MEAM and at most 17% for Tersoff. This may be compared to the 34% superheating that was observed by Broughton and Li during their study of the Stillinger-Weber potential.[38] The liquid configuration that resulted from melting the Tersoff crystal at 3000 K was used as input for the simulation run at 3500 K, and work on the liquid branch of Tersoff silicon began there. Likewise, the MEAM liquid configuration at 2000 K was used as input for simulation at 2500 K. It should be noted that the average densities and energies calculated for the liquid configurations at 3000 K (for Tersoff) and 2000 K (for MEAM) did not depend on whether the initial configuration was solid or high-temperature liquid, indicating that the equilibration times employed for each potential were sufficiently long.

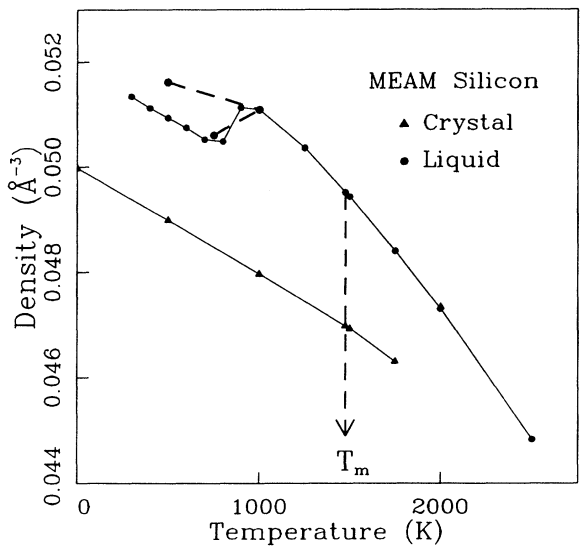

FIG. 6. The density of silicon in the solid and liquid phases as represented by the modified-embedded-atom method. Dashed lines indicate instantaneous quenches to metastable states from an initial temperature of 900 K. Data points on the solid line, which represents the liquid branch at temperatures below 900 K, represent values calculated by cooling the liquid at the rate of 10^{12} K/s, followed by equilibration and averaging. Data were collected along the isobar corresponding to zero average pressure.

The phase diagrams show that both the Tersoff and MEAM yield a liquid silicon phase that is denser than the crystal. This phenomenon, which is observed experimentally, is also reproduced by the Stillinger-Weber potential. The calculated densification at the melting point of MEAM silicon, 1475 K, is 5.4%, which is identical with the experimental value reported in Ref. 38. The calculated densification at the melting point of Tersoff silicon, 2547 K, is 2.0%. Previous work on the Stillinger-Weber potential by Broughton and Li has shown SW to give the densification as 7.7%, which is somewhat too high. The heat of melting may also be obtained from the phase diagrams as the difference in configurational energy between the crystalline and liquid phases at the melting point. This may be done because all systems are at an average pressure of zero. The calculated value of the latent heat for the MEAM is 35.0 kJ/mol, while that of the Tersoff potential is 41.8 kJ/mol, which compares with

the experimental value of 50.6 kJ/mol and the Stillinger-Weber value of 30.9 kJ/mol.

The MEAM predicts the liquid to be between six- and eightfold coordinated, which is in agreement with the Stillinger-Weber potential and with experiment. The calculated coordination number is somewhat dependent on the definition that is used to define a "near neighbor". If a near neighbor is defined as any atom that is within a cutoff shell defined to be the average of the first- and second-neighbor distances in the crystal at the same temperature, then the coordination is reported as six. If the radial distribution function is integrated to the first minimum following the first-neighbor peak, then the value is just above eight. The minimum is shallow, however, only reaching a value of 0.846. The Tersoff potential predicts the liquid to have a first-neighbor coordination at the melting point of between 4.6 and 5.0, although the melting point of the Tersoff potential is much higher than the experimental value. We found that the Tersoff potential produces a liquid with a first minimum in $g(r)$ that reaches a value near 0.25. This value is somewhat smaller than the value of 0.5 found earlier by Tersoff.[20] The structure of liquid silicon predicted by the Tersoff and MEAM potentials is compared to that predicted using the Stillinger-Weber potential and that obtained from neutron-diffraction experiments[42] in Fig. 8. Each curve was obtained at the melting point appropriate for the potential in use. The results show in general that the Stillinger-Weber potential is in reasonable agreement with experiment, although significant differences after the first peak in $g(r)$ are apparent. The Tersoff potential also does fairly well, although the depth of the first minimum is somewhat too deep, as Tersoff has previously reported.[20] The radial distribution function obtained using the MEAM potential does not agree well with experiment, as the density of the liquid is too low with respect to the experimental value. A shoulder in the first peak is also apparent. The relative position of the crystalline and liquid branches produced by the MEAM are satisfactory, however, since the densification on melting is predicted well.

It is also of interest to compare the density of the crystalline phase produced by each of the three potentials considered here with that obtained by experiment. Although study of the liquid phase of silicon is an experimental challenge due to the elevated temperature and corrosive nature of the melt, the properties of crystalline silicon are extremely well known. Figure 9 displays the density of crystalline silicon at zero pressure predicted by the Stillinger-Weber, Tersoff, and MEAM potentials, along with experimental data obtained by two different methods.[43,44] The data show that the Stillinger-Weber potential reproduces the crystalline density well. The Stillinger-Weber density is in error by approximately -0.4% at a temperature of 500 K, and is in error by only -0.04% at a temperature of 1500 K. It should be noted, however, that the Stillinger-Weber potential predicts the curvature of the density vs temperature curve incorrectly. The MEAM and Tersoff potentials do not predict the crystalline density as well as the Stillinger-Weber potential. The MEAM, for example, is in error by -1.7% at a temperature of 500 K. The error in the crystalline density of MEAM silicon grows as the temperature is increased, reaching a value of -4.7% at the melting point of the MEAM. The values for silicon as represented by the Tersoff potential lie between the results for the Stillinger-Weber and MEAM potentials. No evidence was found here that the Tersoff potential yields a negative thermal expansion, as was reported in a previous investigation of the potential.[45]

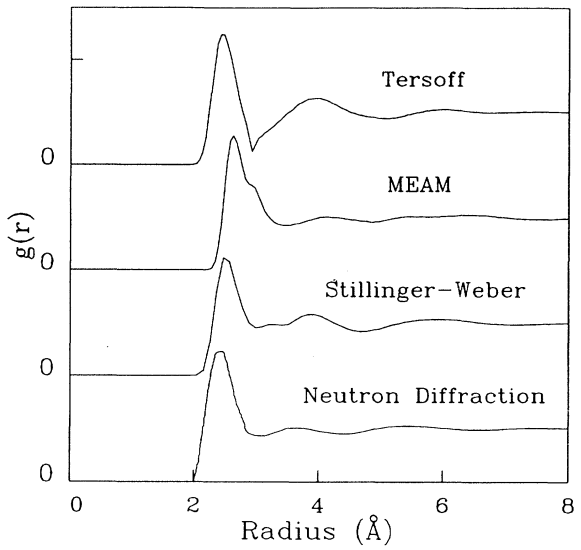

FIG. 8. Radial distribution functions for liquid silicon obtained from molecular dynamics using the MEAM, Tersoff, and SW potentials. Each curve was obtained at the melting point of the respective potential. Hence, the curves do not represent systems at the same temperature.

The heat capacity at constant pressure of each phase

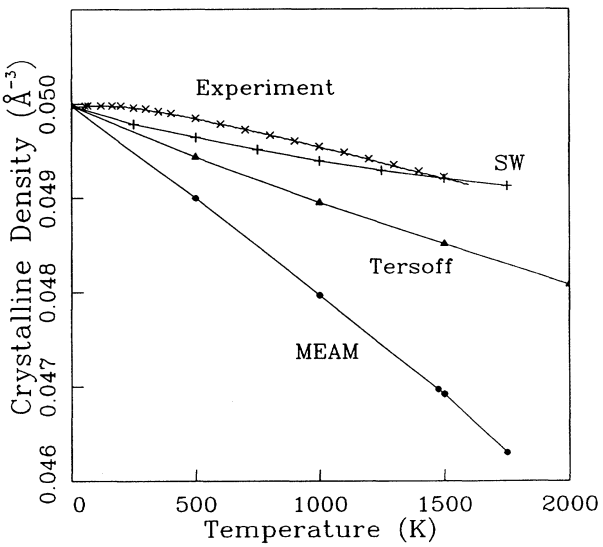

FIG. 9. The temperature dependence of the density of crystalline silicon as represented by three semiempirical potential models.

TABLE I. The properties of silicon at zero pressure as represented by the Tersoff, MEAM, and Stillinger-Weber potential models, as well as the values obtained by experiment. All simulation values are reported at the melting point of the respective potential model.

Property	Tersoff	MEAM	SW[a]	Experiment[a]
Melting point (K)	2547	1475	1691	1683
D_{liquid} (cm^2/s)[b]		1.16×10^{-4}	6.94×10^{-5}	$\sim10^{-4}$
Latent heat_{c-l} (kJ/mol)	4.18	35.0	30.9	50.6
Crystalline density (g/cm^3)[b]	2.218	2.184	2.283	2.40
Liquid density (g/cm^3)[b]	2.263	2.302	2.459	2.53
Liquid coordination	4.6–5.0	6.0–8.2	5.5–6.2	~6.4[c]
Crystalline C_P (J/gK)[b]	1.00	1.08	0.999	1.04
Liquid C_P (J/gK)[b]	1.30	1.15	1.256	1.04
Amorphous density (g/cm^3)[d]	2.291	2.387[e]	2.341[f]	1.71–2.2[g]
Latent heat_{c-a} (kJ/mol)[d]	27.0	23.5[e]	15.4[f]	11.9[h]
Amorphous coordination[d]	4.16	4.65[e]	4.21[f]	4.0–4.25

[a]Reference 38, except where otherwise noted.
[b]Taken at melting temperature of potential model.
[c]Reference 42.
[d]Value at a temperature of 300 K.
[e]It is not clear that the MEAM actually produces *a*-Si.
[f]Reference 47.
[g]Reference 43.
[h]References 54 and 55.

produced by the two potentials has been calculated by a least-squares fit of the enthalpy data obtained by *NPT* molecular dynamics. The values obtained are reported in Table I. Although the MEAM predicts a crystalline density that is much lower than that predicted by either Tersoff or Stillinger-Weber, its description of the heat capacity is comparable to the other two potentials.

The dynamical properties of MEAM liquid silicon have been investigated by calculating the diffusion coefficient at a variety of temperatures between 1000 and 2500 K. The diffusion coefficient of Tersoff liquid silicon was not calculated due to the large difference between the experimental melting point and that predicted by the model.

The diffusion coefficient of MEAM liquid silicon was calculated using a constant volume-constant temperature (*NVT*) molecular-dynamics simulation code. A system size of 100 atoms and a time step of 1 fs were used in this study. Values of the diffusion coefficient were calculated using mean-squared displacement data averaged for 50 ps with averages calculated over 100 time origins to reduce statistical error. The values of the diffusion coefficients so obtained are displayed in Fig. 10, along with a curve fit obtained assuming Arrhenius behavior for the liquid. Least-squares analysis yielded a value of the pre-exponential of 1.54×10^{-3} cm^2/s and an activation energy of 0.33 eV. The fit is quite satisfactory. This may be compared with the Stillinger-Weber values of 3.5×10^{-3} cm^2/s and 0.56 eV, respectively.[46]

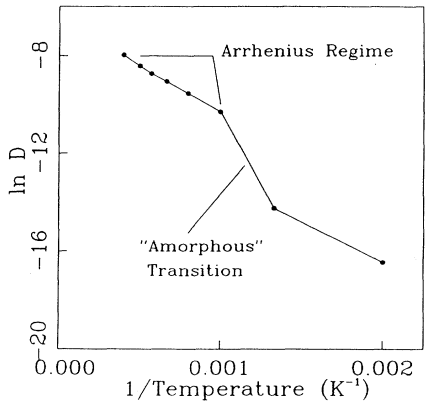

FIG. 10. The temperature dependence of the diffusion coefficient of MEAM liquid silicon.

B. Amorphous phase

The densities of the liquid phase of both the Tersoff and MEAM models for silicon exhibit sudden decreases at temperatures well below the calculated melting points of the potentials. These decreases have been examined with an emphasis on uncovering possible transitions into a phase that approximates amorphous silicon.

The Tersoff potential has been shown previously to yield a phase that resembles amorphous silicon.[20] This phase was attained by instantaneously quenching a liquid configuration at approximately 3000 K to room temperature using a continuous-space Monte Carlo method. This configuration was then annealed for an extended, but unspecified, period of time. The resulting phase had a first-neighbor coordination of approximately 4.25. Continued annealing at negative applied pressures reduced the coordination to 4.09. Tersoff also reports a "significant" reduction in system energy, but does not give the exact value obtained, nor does he report a value

for the density of the amorphous phase produced by his potential. Calculations performed here show that the density of Tersoff silicon decreases substantially as the liquid is instantaneously quenched from 2500 to 2000 K. Further cooling below 2000 K produces a disordered phase that has a density less than that of the solid, but an energy only slightly less than that of the liquid. Examination of the radial distribution function of this phase obtained at 300 K, which is shown in Fig. 11 along with that obtained by Tersoff, shows that the structure of the system obtained here and that obtained by Tersoff are nearly identical. The first-neighbor coordination of the system obtained in this work was obtained by integrating the radial distribution function up to the first minimum. The value obtained at 300 K is 4.16, which lies between the values obtained by Tersoff. The amorphous phase that is obtained is approximately 1% less dense than the crystalline phase at 300 K, and the amorphous phase is approximately 0.28 eV/atom (27.0 kJ/mol) higher in energy than the crystalline phase at 300 K.

An interesting phenomenon occurs in the liquid phase of MEAM silicon at low temperatures in the form of a density maximum that is found at a temperature of 900 K. Instantaneous cooling of the liquid from 1000 K to a temperature of 500 K produced a state point that was a plausible extrapolation of the liquid branch to 500 K. Simulation of a liquid instantaneously quenched from 1000 to 750 K, however, showed a distinct drop in system density below the extrapolation to 500 K. These quenches are shown by dashed lines in Figs. 6 and 7. Broughton and Li had also observed a density maximum when studying the supercooled state of liquid Stillinger-Weber silicon. Their conclusion in 1987 was that the maximum corresponded to a glass transition, whereby the system retained the atomic structure of the liquid but attained a diffusion coefficient appropriate for the solid phase. Luedtke and Landman later suggested, however, that this density maximum actually corresponded to a frustrated phase transition into the amorphous phase.[47] Luedtke and Landman showed that Broughton and Li did not obtain the amorphous phase because they cooled the liquid too quickly, preventing the exploration of phase space necessary to nucleate the amorphous phase.

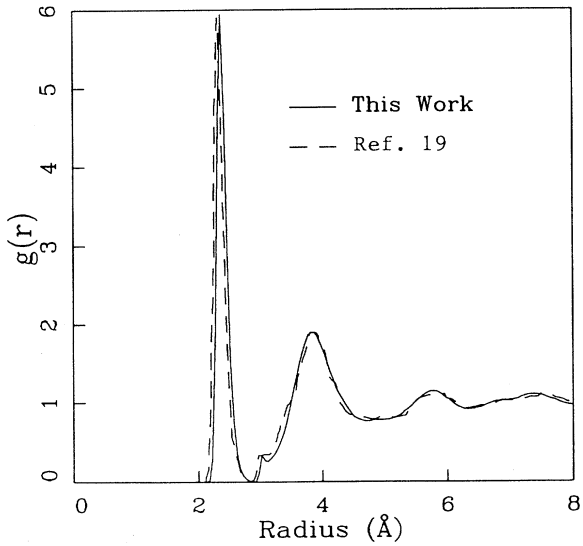

FIG. 11. The radial distribution function of amorphous silicon as represented by the modified-Tersoff potential. Data are presented for a system temperature of 300 K.

The possibility of obtaining a representation of amorphous silicon using the MEAM was examined by performing a series of simulations whereby the liquid phase at 1000 K was slowly quenched to lower temperatures. The configuration at 1000 K was quenched to 900 K at a rate of 10^{12} K/s, and then equilibrated at constant temperature for 50 ps before collecting averages for a further 50 ps. This process was then repeated in intervals of 100 K until the system was at room temperature. This process revealed that the decrease in density occurred between 900 and 800 K, and that further cooling below 800 K produced a smooth, gradual increase in the density from its value at 800 K. These values are shown by the solid line extending to temperatures below 900 K in Figs. 6 and 7. The density at 750 K, obtained from the slower quenching procedure, was found to be lower than that obtained using the instantaneous quench by a modest 0.1%, although the density of the liquid at 500 K predicted using an instantaneous quench procedure was 1.35% higher than that obtained from a slower quenching of the liquid.

The transition between 900 and 800 K was further examined by decreasing the quench rate to a value of 10^{11} K/s. Equilibration and average collection were performed as with the higher quench rate. Although the quench rate had been reduced by an order of magnitude, the resulting system density at 800 K was identical, within the error of the simulation, to the value that was obtained using the higher quench rate. The reversibility of this transition was further probed by heating the 800 K configuration to 900 K at a rate of 10^{12} K/s. Once again, this resulted in identical densities and configurational energies as were obtained from the first quench to 900 K. The stability of the atomic configurations at 800 and 900 K was also probed by holding the systems at their respective temperatures and equilibrating them each for 1 ns of simulation time (10^6 MD time steps each). System densities and energies were calculated in 50 ps segments and as a cumulative average over the 10^6 time steps. Neither system exhibited energy variations between 50 ps intervals greater than 10 meV per system atom, and the density variation between intervals was less than 10^{-3} Å^{-3} for both temperatures. Furthermore, no systematic trend in energy or density was found at either temperature.

The amorphous phases obtained by quenching Tersoff and MEAM liquids may be compared to results that have been obtained for the amorphous phase of the Stillinger-Weber potential.[47] It should be made clear from the outset that the existence of a MEAM amorphous silicon is somewhat in doubt due to the small changes in density and configurational energy that are observed. Table I lists some of the relevant information. Although none of the potentials studied reproduce the experimental results for amorphous silicon accurately, specifically with regard

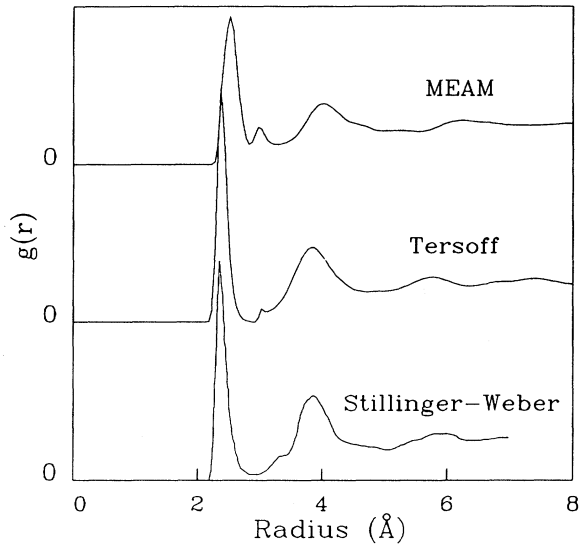

FIG. 12. The radial distribution function of amorphous silicon produced by the Tersoff, MEAM, and SW potentials. All curves represent systems at a temperature of 300 K.

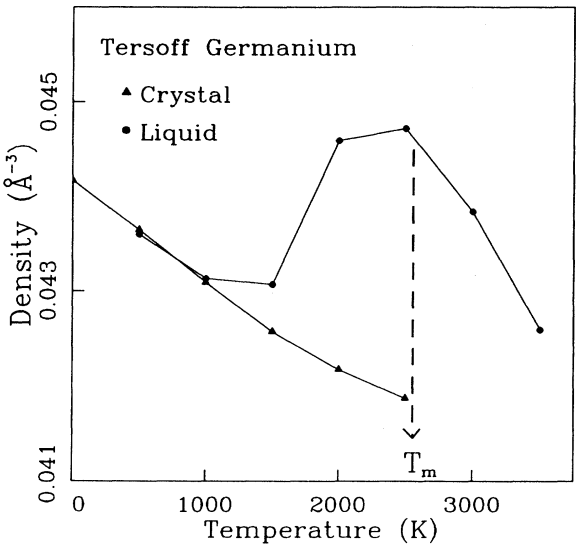

FIG. 13. The density of germanium in the crystalline and liquid phases, as represented by the modified-Tersoff potential. Data were collected along the isobar corresponding to zero average pressure.

to the density, the Stillinger-Weber potential does predict the energetics of the amorphous phase with considerably more accuracy than either Tersoff or the MEAM. The amorphous-crystal latent heat produced by the MEAM, in fact, approaches that predicted by the MEAM for the crystal to liquid transition. The structure of each amorphous phase is presented in Fig. 12, where the radial distribution function obtained from each potential is compared. The first-neighbor coordination for each amorphous phase may be calculated by integrating the radial distribution function up to the first minimum. This procedure has been applied to the functions obtained here for the Tersoff and MEAM potentials to obtain values of 4.16 and 4.65, respectively. Luedtke *et al.* report a coordination for amorphous SW silicon of 4.21. Although the SW and Tersoff results are in reasonable accord, the value obtained from the MEAM potential is somewhat too high. This provides more evidence that the low-temperature disordered phase produced by the MEAM is not representative of amorphous silicon.

V. PHASE DIAGRAMS FOR TERSOFF AND MEAM GERMANIUM

Procedures like those described above were also used to characterize the solid and liquid phases of germanium as described by the Tersoff and MEAM potentials. Results were generally less favorable than those obtained for silicon.

Tersoff germanium was studied using the same method that was used for Tersoff and MEAM silicon. The melting point of Tersoff germanium was determined using the method of Landman *et al.* to be 2554±38 K, which is approximately twice the experimental value of 1210 K. Data for the various phases of Tersoff germanium were obtained using the isothermal-isobaric (*NPT*) simulation code that was developed for the silicon systems. The configurational energies and densities of Tersoff germanium in the crystalline and liquid phases are shown in Figs. 13 and 14. The modified-Tersoff potential predicts a liquid germanium phase that is denser than the crystal at the melting point by approximately 6.8%. This compares well with the experimental value, which is approximately 7.1%,[48,49] although the melting temperature of the Ter-

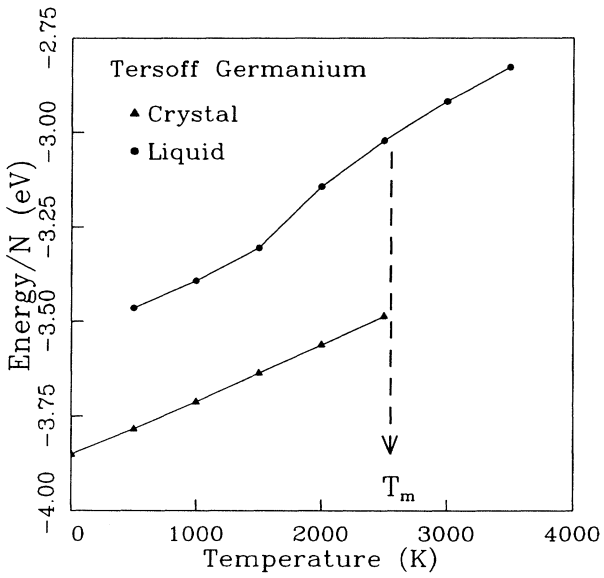

FIG. 14. The configurational energy of germanium in the crystalline and liquid phases, as represented by the modified-Tersoff potential. Data were collected along the isobar corresponding to zero average pressure.

soff system is far above the experimental value. The latent heat of melting was found to be 0.465 eV/atom, or 44.9 kJ/mol. This may be compared to the experimental value of the latent heat, 36.9 kJ/mol.[50] Finally, the room-temperature heat capacity at constant pressure for crystalline germanium was calculated with the Tersoff potential to be 0.37 J/gK. This is in general accord with the experimental value of 0.322.[51]

An attempt was made to determine the melting point of MEAM germanium using the method of Landman *et al.* A crystalline system exposing the (100) orientation to vacuum was created and equilibrated for 50 000 MD time steps at a temperature of 1000 K. Energy was added to the system using the method of energy carriers described in Ref. 39 over a time period of 2 ps. The system temperature rose to approximately 2000 K after the addition of energy, but no melting occurred. Further simulation of this system showed that the crystal was stable at this temperature. An attempt was made to add more energy into the system and the system temperature rose above 2500 K. Significant evaporation of germanium occurred at this temperature without the establishment of a stable liquid phase. It was unknown whether the failure to establish a liquid was due to a weakness of the MEAM germanium potential, or whether energy was added to the simulation cell at a rate that was too great to allow thermal equilibration of the deposited energy. The simulation was, therefore, repeated with a pulse length of 5 ps with a simulation cell whose temperature was 2000 K. The system once again did not melt, but rather, evaporated. A final effort to produce a MEAM germanium system with a solid-liquid interface was carried out by using the equilibrium solid-liquid MEAM silicon system as input. This system had an equilibrium temperature of 1475 K. The identity of the atoms was changed and a constant-energy simulation performed. The liquid quickly began to solidify, causing the system temperature to increase. The temperature reached a value between 2000 and 2500 K in a time of 50 ps. The simulation was halted at this point and efforts to obtain an interfacial MEAM germanium system were abandoned.

The phase diagram of MEAM germanium was studied using the isothermal-isobaric (*NPT*) simulation code that was described in Sec. IV. Heating of crystalline MEAM germanium began at 500 K and continued in increments of 500 K until a temperature of 2000 K was reached. Heating of the crystal was halted at this point, since the system had already superheated significantly with respect to the experimental melting point of germanium, and, since simulations of the interfacial system indicated an instability near 2500 K.

Since previous efforts to produce liquid MEAM germanium failed, an attempt was made to produce the liquid by changing the identity of a bulk MEAM liquid silicon system at a temperature of 1500 K. This system was equilibrated for 50 ps and averages were collected for a further 50 ps. The density and energy that were obtained were plausible values for the liquid, except that the density of the liquid was predicted to be less than that of the diamond crystalline phase. This system was instantaneously heated to 2000 K and the equilibration and

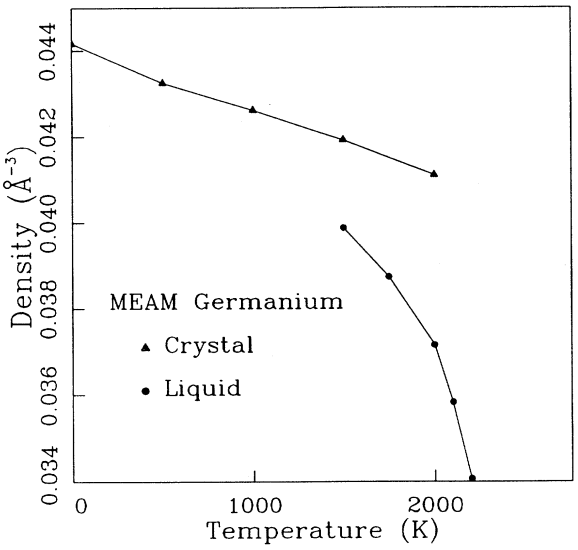

FIG. 15. The density of germanium in the crystalline and liquid phases as represented by the MEAM potential. Data were collected along the isobar corresponding to zero average pressure.

averaging process were repeated. Liquidlike values were once again obtained, with the exception of the density change already noted. Upon instantaneous heating of the system at 2000 K to a temperature of 2500 K, a spontaneous transition to a gaseous state was observed within a time of 100 000 MD time steps (100 ps). In order to remove the possible effect of significant volume fluctuations caused by instantaneously heating the system, data for

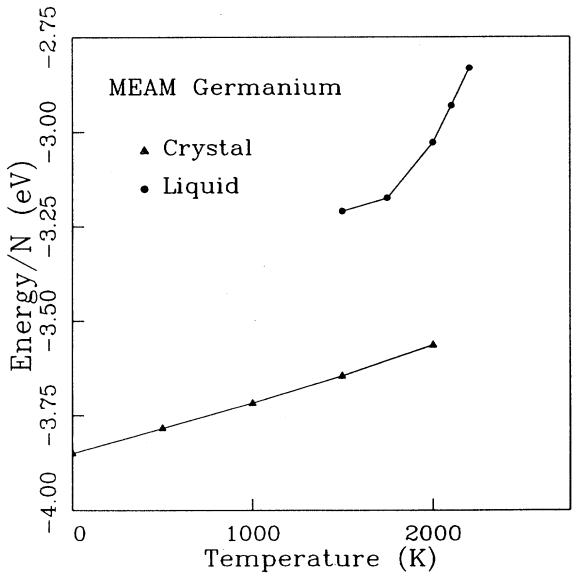

FIG. 16. The configurational energy of germanium in the crystalline and liquid phases as represented by the MEAM potential. Data were collected along the isobar corresponding to zero average pressure.

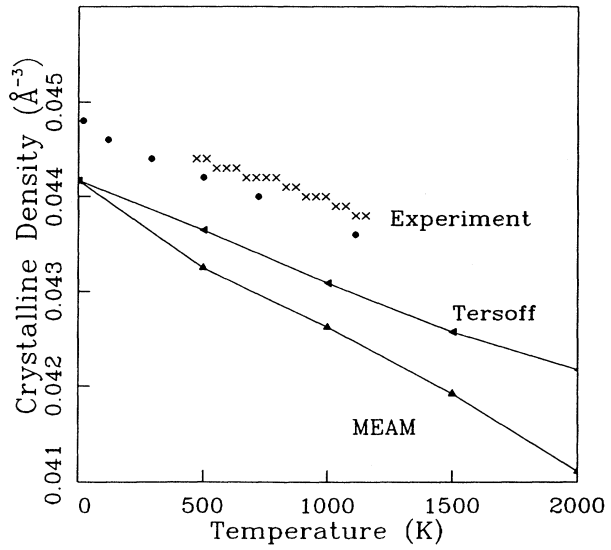

FIG. 17. The temperature dependence of the density of crystalline germanium as represented by the Tersoff and MEAM potentials.

liquid MEAM germanium above 2000 K were obtained by alternately heating the liquid at a rate of 10^{12} K/s for a period of 100 ps, followed by equilibration and averaging at constant temperature for a further 100 ps. Information was then obtained at intervals of 100 K. Slow heating of the liquid resulted in stable configurations at 2100 and 2200 K, but the system spontaneously vaporized during heating to 2300 K. Inspection of the resulting phase diagrams shown in Figs. 15 and 16 suggests that the system at 2200 K might also turn to vapor if a sufficiently long simulation were performed. The apparent difference in quality between the MEAM descriptions of silicon and germanium is puzzling. This difference may be related to the fact that the pair potential portions of MEAM silicon and germanium are not conformal, that is, they are not similar in shape. Although the similarily between silicon and germanium would lead one to expect similarly shaped pair potentials, this is not the case. The origin of this difference in the pair potentials was not investigated.

The density of crystalline germanium predicted by the Tersoff and MEAM potentials can also be compared to experiment. The data, displayed in Fig. 17, show in general that the agreement is no better for germanium than for silicon. The crystalline density given by the MEAM, for example, is in error by -2.2% at 500 K, and increases at higher temperatures. Although the Tersoff potential is more accurate than the MEAM in this regard, it is in error by -1.3% at 500 K.

VI. RAPID SOLIDIFICATION OF MEAM SILICON

The results presented in Sec. VI generally indicate that the MEAM predicts the properties of the solid to liquid transition in silicon fairly well. Although the model seems to be somewhat "underbound," resulting in solid and liquid densities and a melting point that are too low with respect to experiment, the error in most properties is less than 20%. It is of interest then to determine how well the MEAM reproduces aspects of the nonequilibrium solid-liquid interface during a simulation of rapid solidification.

A MEAM silicon system exposing the (100) system was prepared for melting and solidification by equilibrating it at a constant temperature of 1000 K for a period of 50 ps. The temperature scaling was turned off and the system was heated by subjecting it to a beam of energy carriers using the method described in Ref. 39. The intensity of the beam was Gaussian in time, with a density of 0.4 J/cm^2 and a total length of 15 ps. The total absorbed energy density was 3.21 eV/Å^2 (5.14 mJ/cm^2). A total of 2.43 keV (3.89×10^{-16} J) was absorbed. Melting initiated at the vacuum surface and proceeded into the crystal until a maximum melt depth of approximately 32 Å was attained 25 ps after the beginning of the heating process. The interface temperature rose from its initial value of 1000 K during this heating process, reaching a maximum value of approximately 2000 K after 10 ps of heating, or shortly after the maximum intensity of the energy beam was reached at a time of 7.5 ps. The interfacial superheating drove the melting process, causing the interface to cool. The interfacial temperature data were fitted with a least-squares parabola to facilitate analysis. The best-fit temperature at the maximum melt depth, which corresponds to zero interfacial velocity, was found to be 1467 K, which is very close to the equilibrium melting temperature of 1475 K. This indicates good agreement between the melting points determined by the equilibrium simulation methods. As energy was withdrawn from the simulation cell by the heat bath, solidification of the liquid layer began. The liquid was completely crystallized after a time of 115 ps. The melt and temperature history of the sample is shown graphically in Fig. 18, where the melt depth and interfacial temperature are shown as functions of time. The results of two different methods of analysis are shown for the melt depth. The data points, shown as filled circles, are the result of using the radial distribution function and singlet density profile to determine the average position of the interface. The curve is the result of a method whereby the dynamic number of liquid atoms in the system is calculated. The criterion used here to define a "liquid atom" was simply to declare an atom without fourfold coordination to be liquid. Although this definition is not unique, it is another route to the interfacial velocity. The temperature data were acquired using the melt depth calculated from the radial distribution function and density profile. It is apparent from the data that the interface continued to cool during solidification, i.e., no steady-state undercooling was established.

The interfacial velocity was calculated by fitting the melt depth data with a least-squares parabola. The resulting fit is shown in the top graph of Fig. 18 as a solid line. Although the solidification velocity increases continuously as the interfacial undercooling increases, it is clear that the crystal is growing at a rate that is unrealisitically high for (100) silicon. The regrowth velocity at

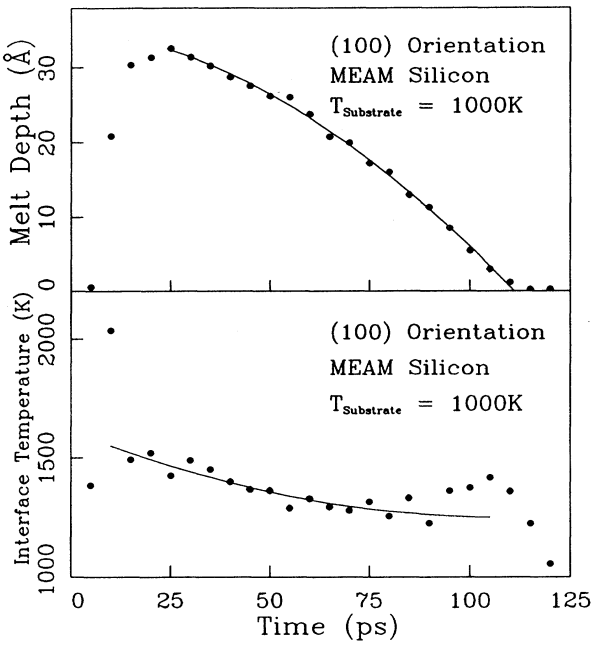

FIG. 18. The melt depth and temperature history of a nonequilibrium molecular dynamics (NEMD) simulation of melting and rapid solidification for MEAM silicon. The temperature shown corresponds to the temperature of those atoms in the interfacial region between solid and liquid.

a time of 80 ps, for example, is 43 m/s. The interfacial temperature at this time is approximately 1275 K, which represents a 200 K or 14% undercooling with respect to the equilibrium melting temperature. At the same percentage undercooling, the Stillinger-Weber potential predicts an interfacial velocity of approximately 15 m/s.[46] Furthermore, the maximum interfacial velocity at which solidification will yield crystalline silicon has been experimentally determined to be 15 m/s.[52,53] Experiments have shown that regrowth above this rate yields the amorphous phase, rather than crystal. Solidification in the MEAM system produced defect-free crystal at a velocity of 43 m/s, which represents a serious error.

The unphysically large solidification velocities observed in the MEAM system may be due to the fact that MEAM silicon has a diffusion coefficient of 1.16×10^{-4} cm^2/s at a temperature of 1475 K, while the corresponding value for Stillinger-Weber is 6.94×10^{-5} at a temperature of 1691 K. The MEAM silicon diffusion coefficient is, in general, twice as large as that predicted by the Stillinger-Weber potential. Since the regrowth velocity is directly proportional to the diffusion coefficient in the Wilson-Frenkel formulation, this accounts for much of the discrepancy between the regrowth velocities using the MEAM and Stillinger-Weber potential model. It should be noted that the larger atomic mobility found in MEAM liquid silicon may be related to the low liquid density predicted by the MEAM.

VII. SUMMARY

The properties of silicon and germanium as modeled by the modified-Tersoff and modified-embedded-atom method have been examined. The properties of crystalline and liquid silicon were found to be adequately modeled by the MEAM, although the level of agreement with experiment was not as good as was obtained previously by Broughton and Li using the Stillinger-Weber potential. Both the crystalline and liquid phases were found to be less dense than is observed experimentally, and the melting point of 1475 K is approximately 14% lower than the experimental value of 1683 K. The latent heat of melting was found to be 35.0 kJ/mol, which compares poorly with the experimental value of 50.6 kJ/mol, but is slightly better than the value of 30.9 kJ/mol predicted by SW. The liquid-phase diffusion coefficient was found to be approximately twice that predicted by the Stillinger-Weber potential, which led to unrealistic resolidification velocities during a nonequilibrium molecular-dynamics simulation of laser melting and regrowth. The MEAM was found to model the amorphous phase of silicon rather poorly. A maximum in the liquid density was found at a temperature of 900 K, but the lower densities that were found by slowly quenching below this value were still substantially greater than those of the crystal at the same temperature. The density of this disordered phase at a temperature of 300 K, for example, was 2.387 g/cm^3, which is too large in comparison to the range of 1.71–2.2 g/cm^3 that is reported for amorphous silicon at this temperature. The coordination of MEAM amorphous silicon is approximately 4.65, which is too large compared with the experimentally observed coordination range of 4.0–4.25.

Although the properties of crystalline silicon are modeled well by the modified-Tersoff potential, those of the liquid phase are not reproduced well. The major error was found to be the predicted melting point of 2547 K, which is approximately 850 K too large. The coordination of Tersoff liquid silicon was found to be approximately 4.6, which is lower than the experimental value of 6–8. The liquid was found to spontaneously nucleate the amorphous phase upon cooling from 2500 to 2000 K. No effort was made to further resolve the transition temperature. The amorphous phase that is obtained upon further cooling to room temperature has a structure that is in general agreement with that produced by the Stillinger-Weber potential. The latent heat of the crystal to amorphous transition at room temperature, however, is 27.0 kJ/mol, which does not compare well with the SW value of 15.4 kJ/mol, nor with the experimental value of 11.9 kJ/mol.

The MEAM potential was found to model the liquid phase of germanium very poorly. Efforts to obtain a stable solid-liquid interfacial system failed, resulting instead in evaporation of the disordered solid. Bulk MEAM liquid germanium was obtained by switching the identity of a moderate temperature MEAM liquid silicon configuration. This system was stable to a temperature of 2200 K, but vaporized during a slow heating of 10^{12} K/s from this value. Although the Tersoff potential was found to produce a stable solid-liquid system for germanium, the predicted melting point of 2554 K compares poorly to the experimental value of 1210 K. The rather poor description of germanium afforded by these two po-

tentials casts serious doubt on their ability to successfully model disordered phases of silicon-germanium alloys.

ACKNOWLEDGMENTS

The authors are pleased to acknowledge the financial support of the National Science Foundation (Grant No. DMR-8915333) and the Cornell Materials Science Center, which is supported by the National Science Foundation (through Grant No. DMR-9121654). We are also pleased to acknowledge a very generous allocation of computer time on a Cray Y-MP from the Pittsburgh Supercomputer Center. S.J.C. wishes to acknowledge helpful discussions with Mike Baskes.

*Current address: Department of Chemical Engineering, University of California, Berkeley, CA 94720-9989.

†Author to whom correspondence should be addressed.

[1]J. R. Abelson, K. H. Weiner, K. B. Kim, and T. W. Sigmon, in *Epitaxy of Semiconductor Layered Structures,* edited by R. T Turg, L. R. Dawson, and R. L. Gunshor, MRS Symposia Proceedings No. 102 (Materials Research Society, Pittsburgh, 1988), p. 323.

[2]J. R. Abelson, T. W. Sigmon, K. B. Kim, and K. H. Weiner, Appl. Phys. Lett. **52**, 230 (1988).

[3]P. M. Smith, S. Lombardo, M. J. Uttormark, S. J. Cook, and M. O. Thompson, in *Evolution of Thin Film and Surface Microstructure,* edited by C. V. Thompson, J. Y. Tsao, and D. J. Srolovitz, MRS Symposia Proceedings No. 202 (Materials Research Society, Pittsburgh, 1991), p. 603.

[4]R. Car and M. Parrinello, Phys. Rev. Lett. **55**, 2471 (1985).

[5]R. Car and M. Parrinello, Phys. Rev. Lett. **60**, 204 (1988).

[6]I. Štich, R. Car, and M. Parrinello, Phys. Rev. Lett. **63**, 2240 (1989).

[7]G. Ackland, Phys. Rev. B **40**, 10 351 (1989).

[8]M. I. Baskes, Phys. Rev. Lett. **59**, 2666 (1987).

[9]M. I. Baskes, J. S. Nelson, and A. F. Wright, Phys. Rev. B **40**, 6085 (1989).

[10]R. Biswas and D. R. Hamann, Phys. Rev. Lett. **55**, 2001 (1985).

[11]R. Biswas and D. R. Hamann, Phys. Rev. B **36**, 6434 (1987).

[12]B. C. Bolding and H. C. Andersen, Phys. Rev. B **41**, 10 568 (1990).

[13]A. E. Carlsson, P. A. Fedders, and C. W. Myles, Phys. Rev. B **41**, 1247 (1990).

[14]J. R. Chelikowsky, J. C. Phillips, M. Kamal, and M. Strauss, Phys. Rev. Lett. **62**, 292 (1989).

[15]E. Kaxiras and K. C. Pandey, Phys. Rev. B **38**, 12 736 (1988).

[16]K. E. Khor and S. Das Sarma, Phys. Rev. B **38**, 3318 (1988).

[17]F. H. Stillinger and T. A. Weber, Phys. Rev. B **31**, 5262 (1985).

[18]J. Tersoff, Phys. Rev. Lett. **56**, 632 (1986).

[19]J. Tersoff, Phys. Rev. B **37**, 6991 (1988).

[20]J. Tersoff, Phys. Rev. B **38**, 9902 (1988).

[21]J. Tersoff, Phys. Rev. B **39**, 5566 (1989).

[22]K. Ding and H. C. Andersen, Phys. Rev. B **34**, 6987 (1986).

[23]M. S. Daw and M. I. Baskes, Phys. Rev. Lett. **50**, 1285 (1983).

[24]M. S. Daw and M. I. Baskes, Phys. Rev B **29**, 6443 (1984).

[25]S. M. Foiles, Phys. Rev. B **32**, 7685 (1985).

[26]S. M. Foiles, Phys. Rev. B **32**, 3409 (1985).

[27]S. M. Foiles, M. I. Baskes, and M. S. Daw, Phys. Rev. B **33**, 7983 (1986).

[28]R. A. Johnson, Phys. Rev. B **37**, 3924 (1988).

[29]R. A. Johnson and D. J. Oh, J. Mater. Res. **4**, 1195 (1989).

[30]R. A. Johnson, Phys. Rev. B **39**, 12 554 (1989).

[31]R. A. Johnson, Phys. Rev. B **41**, 9717 (1990).

[32]D. J. Oh and R. A. Johnson, J. Mater. Res. **3**, 471 (1988).

[33]S. P. Chen, D. J. Srolovitz, and A. F. Voter, J. Mater. Res. **4**, 62 (1989).

[34]M. W. Finnis and J. E. Sinclair, Philos. Mag. A **50**, 45 (1984).

[35]Reference 9 describing the MEAM model contains a misprint. The parameters a^1 and a^2 are switched as reported in the list of parameters. The value of a^1 should actually be used as a^2, and *vice versa.* This is the case for both silicon and germanium.

[36]J. H. Rose, J. R. Smith, F. Guinea, and J. Ferrante, Phys. Rev. B **29**, 1963 (1984).

[37]U. Landman, W. D. Luedtke, R. N. Barnett, C. L. Cleveland, M. W. Ribarsky, E. Arnold, S. Ramesh, H. Baumgart, A. Martinez, and B. Khan, Phys. Rev. Lett. **56**, 155 (1986).

[38]J. Q. Broughton and X. P. Li, Phys. Rev. B **35**, 9120 (1987).

[39]D. K. Chokappa, S. J. Cook, and P. Clancy, Phys. Rev. B **39**, 10 075 (1989).

[40]S. M. Foiles and J. B. Adams, Phys. Rev. B **40**, 5909 (1989).

[41]D. Brown and J. H. R. Clarke, Mol. Phys. **61**, 597 (1984).

[42]Y. Waseda and K. Suzuki, Z. Phys. B **20**, 339 (1975).

[43]Y. Tatsumi and H. Osaki, in *Properties of Silicon,* EMIS Data reviews Series No. 4, INSPEC (The Institution of Electrical Engineers, London, 1988), p. 4.

[44]Y. S. Touloukian, R. K. Kirby, R. E. Taylor, and T. Y. R. Lee, *Thermophysical Properties of Matter* (Plenum, New York, 1977), Vol. 13, p. 154.

[45]W. D. Metzler, M.S. thesis, Air Force Institute of Technology, 1987.

[46]M. H. Grabow, G. H. Gilmer, and A. F. Bakker, in *Atomic Scale Calculations in Materials Science,* edited by J. Tersoff, D. Vanderbilt, and V. Vitek, MRS Symposia Proceedings No. 141 (Materials Research Society, Pittsburgh, 1989), p. 349.

[47]W. D. Luedtke and U. Landman, Phys. Rev. B **40**, 1164 (1989).

[48]*CRC Handbook of Chemistry and Physics,* edited by D. R. Lide (CRC, Ann Arbor, 1991).

[49]E. G. Rochow, in *Comprehensive Inorganic Chemistry,* edited by J. C. Bailar, Jr., H. J. Emeléus, R. Nyholm, and A. F. Trotman-Dickenson (Pergamon, Oxford, 1973), Vol. 2.

[50]J. P. Dismukes and L. Ekstrom, Trans. Metall. Soc. AIME **233**, 672 (1965).

[51]K. K. Kelly (unpublished).

[52]A. G. Cullis, N. G. Chew, H. C. Webber, and D. J. Smith, J. Cryst. Growth **68**, 624 (1984).

[53]M. O. Thompson, J. W. Mayer, A. G. Cullis, H. C. Webber, N. G. Chew, J. M. Poate, and D. C. Jacobson, Phys. Rev. Lett. **50**, 896 (1983).

[54]E. P. Donovan, F. Spaepen, D. Turnbull, J. M. Poate, and D. C. Jacobson, Appl. Phys. Lett. **42**, 698 (1983).

[55]E. P. Donovan, F. Spaepen, D. Turnbull, J. M. Poate, and D. C. Jacobson, J. Appl. Phys. **57**, 1795 (1985).